

1 **1) Title:** Independent evolution of sexual dimorphism and female-limited mimicry in
2 swallowtail butterflies (*Papilio dardanus* and *P. phorcas*)

3

4 **2) Authors:** M.J.T.N. Timmermans^{abe}, M.J. Thompson^{acf}, S. Collins^d, A.P. Vogler^{ab}

5 **3) Affiliations:**

6 a) Department of Life Sciences, Natural History Museum, London, SW7 5BD, United
7 Kingdom

8 b) Department of Life Sciences, Silwood Park Campus, Imperial College London, Ascot,
9 SL5 7PY, United Kingdom

10 c) Department of Zoology, Cambridge University, Downing Street, CB2 3EJ, United
11 Kingdom

12 d) ABRI, P O Box 14308, Westlands 0800, Nairobi, Kenya

13 e) Current address: Department of Natural Sciences, Middlesex University, Hendon
14 Campus, London, NW4 4BT, United Kingdom

15 f) Current address: Peterhouse, Cambridge University, Trumpington Street, CB2 1RD,
16 United Kingdom

17

18 **4) Key words:** Batesian mimicry, phylogenomics, transcriptome, *Papilio phorcas*, sexual
19 selection, polymorphism

20

21 **5) Corresponding author:**

22 Martijn J.T.N. Timmermans

23 m.timmermans@mdx.ac.uk

24

25 **6) Running title:** Polymorphism in *Papilio*

26 **Abstract:**

27 Several species of Swallowtail butterflies (genus *Papilio*) are Batesian mimics that express
28 multiple mimetic female forms, while the males are monomorphic and non-mimetic. The
29 evolution of such sex-limited mimicry may involve sexual dimorphism arising first and
30 mimicry subsequently. Such a stepwise scenario through a non-mimetic, sexually dimorphic
31 stage has been proposed for two closely related sexually dimorphic species; *P. phorcas*, a
32 non-mimetic species with two female forms, and *P. dardanus*, a female-limited polymorphic
33 mimetic species. Their close relationship indicates that female-limited polymorphism could
34 be a shared derived character of the two species. Here we present a phylogenomic analysis
35 of the dardanus group using 3964 nuclear loci and whole mitochondrial genomes showing
36 that they are not sister species, and thus that the sexually-dimorphic state has arisen
37 independently in the two species. Non-homology of the female polymorphism in both species
38 is supported by population genetic analysis of *engrailed*, the presumed mimicry switch locus
39 in *P. dardanus*. McDonald-Kreitman tests performed on SNPs in *engrailed* showed the
40 signature of balancing selection in a polymorphic population of *P. dardanus*, but not in
41 monomorphic populations, nor in the non-mimetic *P. phorcas*. Hence the wing polymorphism
42 does not balance polymorphisms in *engrailed* in *P. phorcas*. Equally, unlike in *P. dardanus*,
43 none of the SNPs in *P. phorcas engrailed* were associated with either female morph. We
44 conclude that sexual dimorphism due to female polymorphism evolved independently in both
45 species from monomorphic, non-mimetic states. While sexual selection may drive male-
46 female dimorphism in non-mimetic species, in mimetic *Papilios* natural selection for
47 protection from predators in females is an alternative route to sexual dimorphism.

48

49 **Introduction:**

50 Conspicuous morphological differences between males and females evident in many
51 species are generally attributed to sexual selection, primarily on male traits (Kraaijeveld
52 2014), but the phenotypic divergence of the sexes may also be driven by natural selection.
53 This was first advocated by A.R. Wallace based on his studies of Southeast Asian butterflies
54 of the genus *Papilio* (Wallace 1865; see also Kunte 2008). Several butterfly species in this
55 genus are prominent examples of male-female dimorphism (Kunte 2009). These species are
56 mostly sex-limited Batesian mimics that gain protection from predation through close
57 morphological similarity with chemically protected models while being not defended
58 themselves (Bates 1862). Mimicry in these species is derived and often limited to the female
59 sex, while the males are non-mimetic (Kunte 2009).

60 Sexual dimorphism is frequently achieved by suppressing male-selected traits in the
61 females (Kraaijeveld 2014). In insects, this is often mediated by sex-specific splice variants
62 of *doublesex* (*dsx*) (see e.g. Kraaijeveld 2014). This locus has been documented to
63 determine sexual dimorphism in the two closely related Southeast Asian swallowtails *Papilio*
64 *polytes* and *P. memnon* (Kunte *et al.* 2014; Nishikawa *et al.* 2015; Komata *et al.* 2016). Both
65 species are sexually dimorphic Batesian mimics that express a mimetic colour morph in
66 females in the presence of the dominant *dsx(H)* allele, whereas homozygous recessive
67 *dsx(h)* females are non-mimetic and resemble the males (Kunte *et al.* 2014; Nishikawa *et al.*
68 2015; Komata *et al.* 2016).

69 The evolution of female-limited mimicry has been hypothesized to evolve through
70 several mutational steps, starting with an initial mutation with female limited effect, for
71 example involving the loss of male selected traits in females. After the evolution of sexual
72 dimorphism, the female-limited phenotype might develop similarity to a toxic model species
73 (Fisher 1927; Nicholson 1927), a process that might be followed by the evolution of
74 additional mimetic forms in sex-limited polymorphic species, either from this initial protected
75 state, or from the ancestral state (Turner 1984). Conversely, female-limitation of the mimetic

76 pattern(s) might also evolve after the evolution of mimicry, perhaps by negative frequency-
77 dependent selection driving the loss of mimicry in males (Kunte 2009). Under the first
78 hypothesis, sexually dimorphic traits first arise because they may be driven by sexual
79 selection, for example exerted by female choice or male-male competition. Under the
80 second hypothesis the dimorphic trait arises because it confers a greater advantage when
81 limited to one sex only, i.e. as a product of natural selection. These different explanations for
82 the causes of sex-limited inheritance of adaptive phenotypes were part of an exchange
83 between Darwin and Wallace (Hoquet & Levandowsky 2016).

84 Phylogenetic reconstruction of closely related species potentially could dissect the
85 evolutionary steps leading to sexual dimorphism and female-limited mimicry. The African
86 Mocker Swallowtail, *P. dardanus*, and its relatives are particularly pertinent to phylogenetic
87 studies of complex phenotypes and the evolution of polymorphic systems (Charlesworth &
88 Charlesworth 1975; Vane-Wright *et al.* 1999; Clark *et al.* 2008; Clark & Vogler 2009). This
89 group includes two sexually dimorphic species, *P. dardanus* and *P. phorcas*. *Papilio*
90 *dardanus* exhibits numerous distinct mimetic female phenotypes throughout the species'
91 range in sub-Saharan Africa (Thompson & Timmermans 2014), which are controlled by a
92 single autosomal locus, termed *H*, that expresses a separate allele for each morph (Clarke &
93 Sheppard 1959, 1960; Clarke & Sheppard 1960). Non-mimetic subspecies also exist in *P.*
94 *dardanus*, specifically *P. d. meriones* and *P. d. humbloti* from Madagascar and the Comoro
95 Islands, in which the female pattern is similar to that of the non-mimetic males ('male-like'
96 females of Clarke & Sheppard 1960). *Papilio phorcas* has two non-mimetic female forms,
97 one of which is similar to the monomorphic males. The two other closely related species
98 within the group are monomorphic, including the non-mimetic *P. constantinus* and the
99 mimetic *P. rex* (Figure 1).

100 Phylogenetic analyses of *P. phorcas* and *P. dardanus* potentially can elucidate the
101 question about the evolutionary path to female-limited polymorphic mimicry (Clarke *et al.*
102 1991; Vane-Wright *et al.* 1999; Clark *et al.* 2008; Clark & Vogler 2009). If both species are

103 found to be sister species, an evolutionary route involving an initial switch to sexual
104 dimorphism would be supported, followed by the subsequent acquisition of mimetic
105 phenotypes in the females (Clarke *et al.* 1991; Vane-Wright *et al.* 1999). Phylogenetic trees
106 based on mitochondrial DNA and nuclear ITS sequences have supported the conclusion that
107 *P. phorcas* and *P. dardanus* are sister species and that *P. constantinus* is their closest
108 relative (Vane-Wright *et al.* 1999; Clark & Vogler 2009; but see Caterino & Sperling 1999),
109 which is consistent with the observation that the two polymorphic species form hybrids in
110 nature (Clarke 1980; Thompson *et al.* 2011); however, this specific phylogenetic
111 arrangement is not supported by data on the nuclear EF-1alpha locus (Vane-Wright *et al.*
112 1999), other nuclear markers (Clark & Vogler 2009), or by combinations of nuclear and
113 mitochondrial loci (Zakharov *et al.* 2004). The common ancestry of female limited
114 polymorphic wing patterning, and hence sexually dimorphism, was favoured by Nijhout
115 (2003) based on presumed commonalities in wing pattern elements across the female forms
116 in both species.

117 In addition to phylogenetic analyses, the increased knowledge about the molecular
118 control of the mimetic polymorphism in *P. dardanus* permits a more direct approach to the
119 question of common ancestry of the female limited polymorphic mimicry system.
120 Associations between female morphs and SNPs in the *engrailed* genomic region suggest
121 that this gene either is the wing pattern (*H*) locus of *P. dardanus*, or is tightly linked to the *H*
122 locus (Timmermans *et al.* 2014). Morph-associated SNPs are organized into highly diverged
123 haplotypes that differ by numerous non-synonymous substitutions, supporting the hypothesis
124 that balancing selection maintains different alleles at this locus within polymorphic
125 populations (Thompson *et al.* 2014; Timmermans *et al.* 2014)

126 A common ancestry for the female-limited polymorphism in the two species would be
127 supported if SNPs in the orthologous *P. phorcas engrailed* region are associated with either
128 of its two morphs, which we here test by association studies. Under such scenario, tests for
129 adaptive evolution might detect a signal of balancing selection in *P. phorcas engrailed*, as

130 has been observed for a polymorphic *P. dardanus* population (Timmermans *et al.* 2014).
131 Also, if balancing selection is the cause of the *engrailed* polymorphism in *P. dardanus*,
132 monomorphic populations, including the male-like *P. d. meriones* race, and the Western
133 African subspecies *P. d. dardanus* which exhibits female-limited mimicry, but is essentially
134 monomorphic for a single mimicry morph (form *hippocoon*) should not show such evidence
135 of selection.

136 We use a phylogenomic approach to re-examine the potential sister relationship of *P.*
137 *dardanus* and *P. phorcas*, including the position of the monomorphic Madagascan
138 subspecies within *P. dardanus*, and conduct a test of adaptive molecular evolution on the
139 *engrailed* locus. The results shed light on the evolutionary progression leading to sexual
140 dimorphism and the acquisition of multiple mimetic phenotypes limited to the females.

141

142 **Material and methods:**

143 **Samples and sequence data**

144 A phylogenomic dataset was constructed by transcriptome sequencing and by shotgun
145 sequencing of total genomic DNA of the members of the dardanus group (*P. rex*, *P. phorcas*,
146 *P. constantinus*, *P. dardanus dardanus*, *P. dardanus tibullus*, *P. dardanus polytrophus*, *P.*
147 *dardanus cenea*, *P. dardanus meriones*; Figure 1). Details on starting material, read length
148 and number of reads generated for each of the libraries are given in Supplementary table
149 S1. Transcriptome data were generated for *P. d. cenea* (from pooled dissected wing discs
150 from pupae), *P. d. dardanus* (thorax), *P. phorcas* (thorax), and *P. constantinus* (pupa). Total
151 RNA was extracted using the Qiagen RNeasy mini kit (*P. d. cenea*) or the Qiagen RNA kit
152 (the other samples). Residual DNA was removed with Ambion Turbo DNA-free
153 (Thermofisher). Quality checks and quantification of extracted RNA was assessed using
154 agarose gel electrophoreses, on a Qubit 2.0 Fluorometer and using a RNA chip on a
155 Bioanalyzer (Agilent). Sequencing libraries were sequenced on the Illumina GAIIx (*P. d*

156 *cenea*; 50bp single-end sequencing) or MiSeq (other samples; 250bp paired-end
157 sequencing) platforms.

158 Whole genome shotgun sequence (WGS) data were generated for *P. rex* and four
159 additional subspecies of *P. dardanus* (Supplementary table S1; Figure 1). DNA was
160 extracted from a small piece of thorax using the Qiagen Blood and Tissue kit. The protocol
161 was modified slightly in that ATL buffer was replaced with a cetyltrimethylammonium
162 bromide (CTAB) buffer (2% CTAB (weight/volume), 100 mM Tris-HCl (pH 8.0), 20 mM
163 EDTA, 1.4 M NaCl). Prior to adding buffer AL, the CTAB solution was treated with an equal
164 volume of chloroform:isoamyl alcohol (24:1) to remove protein. Sequencing libraries were
165 sequenced on the Illumina GAIIX (100bp paired-end sequencing) or MiSeq (250bp or 300bp
166 paired-end sequencing) platforms. Two further *Papilio* sequence datasets were downloaded
167 from the GenBank SRA database (*P. glaucus* - SRR850325 and *P. polytes* - SRR850327;
168 Zhang *et al.* 2013).

169 The GAIIX transcriptome reads (*P. d. cenea*) were assessed using FastQC
170 (<http://www.bioinformatics.babraham.ac.uk/projects/fastqc/>) and error-corrected using
171 Reptile (MacManes & Eisen 2013; Yang *et al.* 2010). All other data were processed using
172 the prinseq-lite perl script (Schmieder & Edwards 2011) using the following settings:
173 exact_only, derep: 14, min_qual_mean: 20, ns_max_n: 0, trim_qual_right: 30.

174

175 **Transcriptome and genome assembly and non-redundant reference set**

176 The *P. d. cenea* GAIIX data was assembled using Trinity (version 2013-11-10 release;
177 Grabherr *et al.* 2011). A range of parameters was tested for the *minimum kmer coverage*
178 and *path reinforcement distance* parameters to obtain the highest mean and median contig
179 length. Only contigs of more than 200 bp were retained for further analysis. Completeness of
180 the assembly was assessed using CEGMA (Parra *et al.* 2007; Parra *et al.* 2009). A non-
181 redundant reference sequence set was generated with CD-hit (Li & Godzik 2006) using the
182 following settings: C= 0.95 n=0.8 r=1. This dataset was then parsed through HaMStR

183 (Ebersberger *et al.* 2009) to remove putative paralogous sequences using the LEP1-Cos
184 ortholog set (Kawahara & Breinholt 2014) with *H. melpomene* as reference. HaMsTr selects
185 best hits to a reference set and concatenates partial hits to increase total sequence length
186 for each locus.

187

188 **Phylogenomic analyses**

189 The reference transcriptome pruned by HaMsTr was used for phylogenetic analyses. To
190 obtain presumed homologous sequences for each of the other (sub)species, the quality
191 controlled and de-replicated sequence reads were mapped onto the non-redundant
192 transcriptome reference set using BWA mem (<http://bio-bwa.sourceforge.net/bwa.shtml>)
193 (default settings). To allow for the more divergent reads of the outgroups to be mapped, the
194 *P. polytes* and *P. glaucus* reads were aligned using the short read aligner BBmap
195 (<http://sourceforge.net/projects/bbmap/>) (setting: local=t), which is more tolerant to sequence
196 divergence than BWA. SAM files were converted to sorted BAM files using Samtools (Li *et*
197 *al.* 2009), and Picard (v.1.117) (<http://broadinstitute.github.io/picard/>) was used to add read
198 group information. GATK (<https://www.broadinstitute.org/gatk/>) was used to call sites
199 different to the reference sequence (in homozygous and heterozygous states). All sites were
200 emitted into a vcf (<https://github.com/samtools/hts-specs>) file, which was subsequently
201 converted into fasta formatted sequences using a custom Perl script.

202 The information on the different specimen was combined into a multi-fasta alignment
203 file. These files were subsequently combined into a single concatenated data matrix. The
204 number of positions that were homozygous and differed from the *P. d. cenea* reference
205 sequence was determined for each specimen and comparisons were made after correcting
206 for missing data by dividing this number by the fraction of available data.

207 For phylogenetic analysis, positions with missing data for any of the biological samples
208 were subsequently discarded and individual multi-fasta alignments with a final length <100
209 were removed. To obtain a suitable partitioning scheme, the alignment was analysed using

210 PartitionFinder (Lanfear *et al.* 2012) (starting with one partition per non-redundant transcript
211 fragment) based on the Bayesian Information Criterion (BIC). The partitioned data matrix
212 was subsequently used for Maximum Likelihood (ML) based phylogenetic analysis. Analyses
213 were performed in RAxML (Stamatakis 2006) and used a GTR+ Γ model for each partition. In
214 addition, RAxML trees were generated for each of the individual alignments, again using the
215 GTR+ Γ model for each of the datasets. Branch lengths were removed from these individual
216 phylogenetic trees ('best trees') using newick-utils (v.1.6) (Junier & Zdobnov 2010) and a
217 "Densitree" tree plot (Bouckaert 2010) was created in R (<https://www.r-project.org/>) using the
218 packages ape (Paradis *et al.* 2004) and phangorn (Schliep 2011).

219 In addition, full mitochondrial genomes were obtained for eight specimens of the
220 dardanus group, either by LR-PCR (*P. d. dardanus* (Uganda), *P. phorcas*, *P. constantinus*,)
221 following (Timmermans *et al.* 2014b), by assembly from sequenced total DNA (*P. d.*
222 *dardanus* (Ghana)) as described in Gillett *et al.* (2014), or were retrieved from the above
223 WGS datasets (*P. d. tibullus*, *P. d. polytrophus*, *P. d. meriones*, *P. rex*) by assembling the full
224 dataset using Newbler (Margulies *et al.* 2005) and BLAST-based (Altschul *et al.* 1990)
225 identification of the mitogenome sequence from the resulting contigs based on sequence
226 similarity to an existing *P. dardanus* mitogenome sequence (JX313686; Timmermans *et al.*
227 2014). Finally, an incomplete mitogenome sequence for *P. d. cenea* was obtained by
228 mapping transcriptome reads to the existing *P. dardanus* mitogenome using Geneious R8
229 (Kearse *et al.* 2012). The data on the nine newly generated mitogenome sequences were
230 merged with seven existing mitogenomes (the existing *P. dardanus* sequence and six
231 outgroup species) obtained from NCBI GenBank. Sequences of the protein coding and rRNA
232 genes were extracted using FeatureExtract (Wernersson 2005), aligned with Transalign
233 (Bininda-Emonds 2005) for protein coding genes and MAFFT (Kato *et al.* 2009) for rRNA
234 genes (E-INS-i algorithm), and combined into a single multigene data matrix. Tree searches
235 were conducted on all positions or after masking synonymous positions in alignments of
236 protein coding genes using the Degen script (Regier *et al.* 2010; Zwick *et al.* 2012).

237 PartitionFinder (Lanfear *et al.* 2012) was used to select a suitable partition scheme (starting
238 with one partition per codon-position per gene) based on the BIC. Maximum likelihood tree
239 searches were conducted with RAxML using a GTRCAT model for each partition.

240

241 **Molecular evolution of wing-pattern candidate *engrailed***

242 Population-level analyses were conducted by sequencing a 424 bp portion of the *engrailed*
243 coding region amplified with primers Pd202-Pd204 (Thompson *et al.* 2014) for *P. phorcas*
244 (Kenya; Mount Kenya, specimen collected June 2014) and three subspecies of *P. dardanus*,
245 including the East African *P. d. polytrophus* (Kenya; Mount Kenya, specimen collected in
246 June 2014), the West African *P. d. dardanus* (Ghana; Aburi Botanical Gardens, specimen
247 collected in March 2012) and the monomorphic *P. d. meriones* (Madagascar; obtained at
248 various sites and times). Fragments were bi-directionally sequenced using Sanger
249 technology. For each (sub)species a gene alignment was generated. Haplotypes were
250 inferred using the “phase” algorithm in DnaSP v5 (Librado & Rozas 2009) using default
251 settings. Inferred haplotypes were combined with data on three *P. rex* specimens
252 (KJ458896, KJ458897 and the specimen described above) or four *P. constantinus*
253 specimens (KJ458933, KJ458919, KJ458894, KJ458895) and the number of synonymous
254 differences per synonymous site was calculated for each alignment using the Nei-Gojobori
255 model (Nei & Gojobori 1986) in MEGA6 (Tamura *et al.* 2013). In order to detect signatures of
256 selection, McDonald-Kreitman (McDonald & Kreitman 1991) tests were performed on each
257 population sample using the MKT webserver (Egea *et al.* 2008) using default settings. For
258 this, Jukes and Cantor (Jukes & Cantor 1969) corrections were applied. We also reanalysed
259 data on *engrailed* from a population on Mount Kenya that was used for a previous MK test
260 and that earlier had used *P. polytes* and *P. glaucus* for comparison (Timmermans *et al.*
261 2014). Timmermans *et al.* (2014) used a different reverse primer resulting in a 407bp
262 fragment included here. Finally, Fisher’s exact tests were performed to test whether SNPs

263 in *engrailed* are associated to wing phenotype in *P. phorcas*. Bonferroni corrections were
264 applied to correct for multiple testing for these Fisher's exact tests.

265

266 **Results:**

267 **Generating a phylogenomic data set**

268 Illumina sequence data for seven specimens (Supplementary Table S1) ranged from ~5M to
269 50M reads. Quality filtering removed between 2% and 53% of the reads, mostly because
270 reads were redundant, i.e. exact duplicates in particular in the RNA-seq datasets. A similar
271 redundancy was seen in the two publicly available datasets of *P. glaucus* and *P. polytes*
272 obtained from the SRA database, which included between 54% and 58% of redundant
273 reads. Redundancy in the WGS datasets was significantly lower with a maximum of 12% for
274 sample BMNH1043081 (*P. d. tibullus*). The Trinity wing disc transcriptome assembly was
275 composed of 29184 contigs. The transcriptome was assessed for completeness against 248
276 core eukaryotic genes, which suggested the data is 95.5% complete and 98.7% complete if
277 partially assembled genes were included.

278 CD-hit reduced the dataset to a non-redundant sequence set of 27489 contigs, which
279 were compared to the custom ortholog set of 6568 loci of Kawahara & Breinholt (2014) using
280 *H. melpomene* as reference. The HMM based HaMSTR pipeline identified 5408 putative
281 homologues in the non-redundant wing transcriptome set. These loci were used for further
282 phylogenomic analyses and homologous sequences were obtained for the seven *dardanus*
283 group specimens and two outgroups by mapping reads onto the transcriptome reference set.
284 Overall coverage obtained with each of the samples is given in supplementary figure S1.
285 The gDNA based sequence sets showed a significant percentage of positions having a
286 coverage >10x. Sequence coverage of the three RNA-seq samples was generally much
287 lower.

288

289 **Phylogenetic analyses**

290 For each of the ten taxa (*P. d. cenea* reference + 7 *P. dardanus*-species group + 2
291 outgroups) sequences for the 5408 loci were merged into a concatenate of 7,387,602 bp.
292 The number of positions that were homozygous and differed from the *P. d. cenea* reference
293 sequence was counted for each specimen (Figure 2). As expected, the number of such sites
294 increased with phylogenetic distance. Sites with missing data were subsequently removed
295 and loci with a total length of 99 bp or less were also discarded, for a final set of 3964 loci
296 (with a total length of 2,564,740 bp). Maximum Likelihood trees were obtained for each of
297 these loci, as well as for the concatenated dataset (Figure 3). The latter analysis produced
298 topologies with high bootstrap values and support the sister relationship of *P. constantinus*
299 and *P. dardanus*, with *P. phorcas* as sister to both of them. It also indicated that *P. d.*
300 *meriones* split at the basal node of the *P. dardanus* lineage. Phylogenetic analyses of
301 mitogenomes revealed the same topology as obtained with the nuclear dataset, with *P.*
302 *constantinus* as sister to *P. dardanus* and the more distant position of *P. phorcas* (Figure 4).
303 Within *P. dardanus* the placement of *P. d. meriones* remained uncertain based on the
304 mitogenomes, as it was grouped with the West African population but with low bootstrap
305 support, while it was well separated from the polymorphic Eastern African populations.

306

307 **Molecular evolution of *engrailed* and association with *P. phorcas* phenotypes**

308 McDonald-Kreitman (MK) tests were performed on four population samples, including the
309 highly polymorphic East African *P. d. polytrophus* (Kenya) (n=67; all females), the West
310 African *P. d. dardanus* (Ghana) (n=13; all males), the monomorphic *P. d. meriones*
311 (Madagascar) (n=13), and the polymorphic *P. phorcas* (Kenya) (n=15; all females, 8 of which
312 exhibiting the male-like phenotype). In addition, data on *P. d. polytrophus* (Kenya) from an
313 earlier study was reanalysed (Timmermans *et al.* 2014) (Table 1). The *P. d. polytrophus*
314 (Kenya) population datasets, with multiple mimetic forms, showed a significant excess of
315 polymorphic non-synonymous mutations in *engrailed*, consistent with long-term balancing
316 selection (Nielsen 2005). The tests were not significant for the monomorphic *P. dardanus*

317 datasets from Ghana and Madagascar, or for *P. phorcas*, which has dimorphic, but non-
318 mimetic females. A total of 29 SNPs were observed in the *P. phorcas* alignment, and after
319 Bonferroni correction none of these were significantly associated to either of the two female
320 phenotypes.

321

322 **Discussion:**

323 Understanding the relationship of *P. dardanus* and *P. phorcas* is considered critical for
324 understanding the evolution of female-limited polymorphic mimicry (Vane-Wright *et al.* 1999).
325 Although such phylogenetic analysis does not provide direct evidence for the evolution of the
326 colour polymorphism itself, a sister relationship of these female-limited polymorphic species
327 may indicate the antiquity of this trait and thus support the evolution of female-limited
328 polymorphic mimicry in *P. dardanus* from an ancestor that was already sexually dimorphic
329 (Nijhout 2003). More distant relationships of the two species would indicate that sexual
330 dimorphism has arisen independently, possibly through the evolution of a sexual
331 monomorphic, mimetic state in *P. dardanus*, followed by the secondary loss of mimicry in the
332 males (e.g. Kunte 2009; Vane-Wright 1971). Our phylogenetic analysis does not support the
333 hypothesis of a common origin of sexual dimorphism. Separate gains are also corroborated
334 by the non-homologous mechanism of engrailed involvement, which is evident from the fact
335 that the female polymorphism is not associated to variation in *engrailed* in *P. phorcas*, unlike
336 in *P. dardanus*, and that the signature of balancing selection in *engrailed* was missing from
337 *P. phorcas*, but was clearly evident in the polymorphic populations of *P. dardanus*. These
338 results for the dardanus group are in accordance with the phylogenetic study of Kunte (2009)
339 who found no evolutionary correlation of sexual and mimetic dimorphism generally in the
340 genus *Papilio*. However, strictly speaking, we cannot exclude a scenario in which the
341 ancestor of the whole clade was sexually dimorphic, with *P. constantinus* and *P. d. meriones*
342 subsequently losing sexual dimorphism. If so, female-limited polymorphisms would have
343 evolved secondarily, given the non-homology of the *P. phorcas* and *P. dardanus*

344 phenotypes, but this scenario is entirely hypothetical and not supported by any specific
345 evidence.

346 The independent origins of the female limited mimetic polymorphisms in various
347 Papilios (Kunte 2009) might suggest a different underlying genetic basis in each mimetic
348 species. The recent discovery that *dsx* acts as the switch locus in two Southeast Asian
349 swallowtails *P. polytes* (Kunte *et al.* 2014; Nishikawa *et al.* 2015) and *P. memnon* (Komata *et*
350 *al.* 2016) is intriguing, especially as sequence analysis suggests that the mimetic
351 polymorphism evolved independently in both species. Yet, the lack of involvement of
352 *engrailed* in those species, supports the non-homology of the polymorphic mimicry systems
353 across the wider genus *Papilio*. For *P. phorcas*, the morph-determining locus remains
354 unknown, but all evidence obtained here argues against the involvement of *engrailed*.

355 Any hypothesis for the evolution of mimetic forms in *P. dardanus* has to take into
356 account that the evolution of male and female patterns is uncoupled, and potentially involves
357 different mechanism; *engrailed* determines the female morph, but it may not determine the
358 sexual dimorphism *per se*, while *vice versa* we do not know what role *engrailed* plays in
359 determining the male pattern, and if it has a role at all. The male patterns in both *P.*
360 *dardanus* and *P. phorcas* are curious because they are very different from each other and
361 also differ greatly from the presumed ancestral yellow-banded pattern in *P. constantinus* and
362 other related species (Figure 1). This suggests a shift to derived, but non-mimetic male
363 phenotypes in each case, possibly driven by sexual selection, as pointed out by Nijhout
364 (2003).

365 Molecular analyses may inform in greater detail about the separate determination of
366 female morph and male-female dimorphism. In the single case of *P. polytes* studied to date,
367 maleness appears to be achieved by suppressing the female phenotype. Specifically, RNAi
368 knockdown experiments that silenced the dominant *dsx* allele in *P. polytes* showed that this
369 allele not only specifies the mimetic female pattern but at the same time suppresses the non-
370 mimetic (male-like) phenotype (Nishikawa *et al.* 2015), supporting a dual function of the

371 mimicry *H* alleles in specifying the female morph and the sexual dimorphism. In analogy, the
372 specification of the female morph in *P. dardanus* is through *engrailed*. However, the sexual
373 dimorphism might be determined by a different locus, whose identity we don't know, but
374 based on its role in other insects (Kraaijeveld 2014) could quite possibly be the *dsx* locus.

375 This hypothesis about what determines male patterns also bears on the question
376 about the *H* status of the male-like females in *P. dardanus* and their evolution. If the male-
377 like females result simply from suppression of maleness, a mutational loss-of-function in the
378 male-suppressing locus would produce a male-like phenotype in the females, i.e. male-like
379 females could have evolved secondarily. This possibility is unlikely for the monomorphic
380 Indian Ocean subspecies *P. d. meriones* that apparently express the plesiomorphic state
381 (sexual monomorphism) of the *P. dardanus* lineage. A male-like female phenotype, however,
382 is also found in several polymorphic African mainland populations (Clarke & Sheppard 1960;
383 Thompson & Timmermans 2014), which may have originated from reversals, by losing the
384 repression of the mimicry male phenotype due to a mutation in the male-suppressing locus.
385 Importantly, in both cases the male pattern is not a springboard from which female forms
386 diversify.

387 Taken together, current evidence reinforces the general notion that the mimetic
388 patterns are derived and the male pattern is ancestral. Initially Clarke *et al.* (1985) inferred
389 the ancestry of the male patterns based on wing pattern dominance hierarchies. As
390 expected for an ancestral phenotype, crosses performed by these authors revealed that the
391 male pattern (as displayed by male-like females) was recessive to the other female forms in
392 most cases (Clarke *et al.* 1985). There may be problems with the interpretation of these
393 dominance patterns, in particular involving crosses between the monomorphic Malagasy and
394 polymorphic African mainland individuals, because the phenotypes in the offspring are not
395 expressed cleanly. However, together with the increasingly better understanding of the
396 underlying genetic mechanism, including RNAi experiments in *P. polytes* (Nishikawa *et al.*
397 2015) showing the suppression of maleness via the presumed derived *dsx* alleles, there is

398 sufficient evidence for the non-mimetic state to be plesiomorphic, which is retained in the
399 males, and from which the mimicry pattern is derived only in the females driven by natural
400 selection for the avoidance of predation. This does not mean, however, that the male
401 pattern cannot undergo changes also, as is clearly the case in *P. dardanus* and *P. phorcas*
402 whose males do not resemble the presumed ancestral form (Vane-Wright et al. 1991).

403 The alternative possibility for the evolution of sexual dimorphism driven by sexual
404 selection on the male phenotype seems to be refuted for *P. dardanus*, and also seems less
405 common based on the phylogenetic reconstructions of male and female-limited traits in other
406 (non-mimetic) butterflies (Oliver & Monteiro 2011). However, the case of *P. phorcas*, which
407 differs in particular by the absence of mimicry, may yet be explained by the divergence of
408 males, possibly driven by sexual selection, from which females are secondarily derived with
409 similar male-like phenotypes.

410

411

412 **Acknowledgements:**

413 The authors would like to thank Ashanti African Tours, S. Sáfián (Butterfly Conservation
414 Ghana), L. Kirkpatrick and O. Brattström for help with sampling of butterflies and/or for
415 providing butterfly tissue and R. Massang for very kindly granting permission to collect *P.*
416 *dardanus* in Aburi Botanical Gardens (Republic of Ghana). The authors also thank C. Jiggins
417 for constructive discussions on transcriptome assembly and phylogenomic analysis and K.
418 Kraaijeveld, J. Paps and two anonymous reviewers for their valuable comments on our
419 manuscript. The NHM London and NBAF Edinburgh generated sequencing libraries and
420 performed the Illumina sequencing. This study was funded by NERC Postdoctoral
421 Fellowship NE/I021578/1 (to MJTNT), NERC NE/F006225/1 (to APV), and a NERC doctoral
422 fellowship to MJT.

423

424 **Data Accessibility:**

425 All Illumina sequence datasets are stored in the Short Read Archive
426 (<http://www.ncbi.nlm.nih.gov/sra>) under accession numbers SAMN05819004-
427 SAMN05819010. Sanger sequences and newly generated mitochondrial genomes have
428 been deposited in NCBI GenBank under accession numbers KX034410-KX034516 and
429 KX033351-KX033358.

430

431 **Author Contributions:**

432 Designed the study: MJTNT, MJT, APV. Collected material: SC. Analysed the data: MJTNT,
433 MJT. Wrote manuscript: MJTNT and APV. All authors read and approved the final version of
434 the manuscript.

435

436

437 **Figure legends:**

438

439 **Figure 1:** A) Species of the *dardanus* group in the current study, including the two
440 polymorphic species *P. phorcias* and *P. dardanus*. The male of *P. dardanus* is shown in the
441 bottom left corner. Male(-like) pattern of *P. phorcias* are shown on the left. B) The
442 geographical distribution of the five subspecies of *P. dardanus* that were analysed.

443

444 **Figure 2:** The number of positions (x1000) that differed from the *P. d. cenea* reference
445 sequence and were homozygous. Uncorrected: direct count, a total of 7,387,602 sites were
446 investigated, positions with missing data were ignored. Corrected: Number corrected by
447 dividing it by the fraction of missing data. A) Intraspecific comparisons, B) interspecific
448 *dardanus* group comparisons, C) comparisons with outgroups.

449

450 **Figure 3:** A) Densitree graph visualising 3964 Maximum Likelihood phylogenetic trees (one
451 for each transcript fragment). B) Maximum Likelihood tree based on concatenated dataset
452 with no missing data (2,564,740 bp). Bootstrap values are shown on nodes. Scale bar
453 indicates expected changes per site.

454

455 **Figure 4:** Phylogenetic relationships within the *dardanus* group based on full mitochondrial
456 genomes. Bootstrap values are shown on nodes. Scale bar indicates expected changes per
457 site.

458

459

460 **Tables:**

461

462 **Table 1:** Distances and McDonald-Kreitman test for the engrailed locus. Results from
463 analyses with *P. rex* and *P. constantinus* are given for each (sub-)species. Divergence is
464 defined as the number of (non-)synonymous differences per (non-)synonymous site. For the
465 McDonald-Kreitman tests (MK test) synonymous and non-synonymous differences (fixed
466 and variable) after Jukes and Canter (Jukes & Cantor 1969) correction are given. N)
467 Number of specimen. (*) Data from Timmermans et al. 2014). (**) Female form *P. dardanus*
468 f. *dionysos* occurs at low frequency in this population

469

470 **Supplementary data:**

471 **Supplementary Table S1:** Detailed information on sequence datasets, including read
472 length, number of sequences and Quality Control. Paired reads were generated and the first
473 column in each field refers to the forward reads (R1) and the second column to the reverse
474 reads (R2). Dataset SRR850325 and SRR850327 from Zhang *et al.* (2013).

475

476 **Supplementary Figure S1:** Percentage of bases in the transcriptome dataset with the
477 coverage given on the x-axis. For each of the nine sequence sets the reads were mapped
478 onto the non-redundant wing transcriptome dataset and coverage information was obtained
479 using Samtools “depth” function.

480

481

482 **References:**

- 483 Altschul SF, Gish W, Miller W, Myers EW, Lipman DJ (1990) Basic local alignment search tool. *Journal*
484 *of molecular biology*, **215**, 403–410.
- 485 Bates HW (1862) Contributions to an insect fauna of the Amazon valley. Lepidoptera: Heliconidae.
486 *Transactions of the Linnean Society London*, **23**, 495–566.
- 487 Bininda-Emonds ORP (2005) transAlign: using amino acids to facilitate the multiple alignment of
488 protein-coding DNA sequences. *BMC bioinformatics*, **6**.
- 489 Bouckaert RR (2010) DensiTree: making sense of sets of phylogenetic trees. *Bioinformatics*, **26**,
490 1372–1373.
- 491 Caterino MS, Sperling FAH (1999) Papilio phylogeny based on mitochondrial cytochrome oxidase I
492 and II genes. *Mol Phylogenet Evol*, **11**.
- 493 Charlesworth D, Charlesworth B (1975) Theoretical genetics of Batesian mimicry. 2. Evolution of
494 supergenes. *Journal of Theoretical Biology*, **55**, 305–324.
- 495 Clarke CA (1980) *Papilio nandina*, a probable hybrid between *Papilio dardanus* and *Papilio phorcas*.
496 *Systematic Entomology*, **5**, 49–57.
- 497 Clarke CA, F. M. M. Clarke, S. C. Collins, A. C. L. Gill, J. R. G. Turner (1985) Male-like females, mimicry
498 and transvestism in swallowtail butterflies. *Systematic Entomology*, **10**, 257–283.
- 499 Clarke SC, I. J. Gordon, R. I. Vane-Wright, C. R. Smith (1991) Phylogenetic relationships of three
500 African swallowtail butterflies, *Papilio dardanus*, *P. phorcas* and *P. constantinus*: new data
501 from hybrids (Lepidoptera: Papilionidae). *Systematic Entomology*, **16**, 257–273.
- 502 Clarke CA, P. M. Sheppard (1959) The genetics of *Papilio dardanus* Brown. I. Race *cenea* from South
503 Africa. *Genetics*, **44**, 1347–1358.
- 504 Clarke CA, P. M. Sheppard (1960) The genetics of *Papilio dardanus* Brown. II. Races *dardanus*,
505 *polytrophus*, *meseres*, and *tibullus*. *Genetics*, **45**, 439–456.
- 506 Clarke CA, Sheppard PM (1960) The genetics of *Papilio dardanus* Brown. III. Race *antinorii* from
507 Abyssinia and race *meriones* from Madagascar. *Genetics*, **45**, 683–698.

508 Clark R, S. M. Brown, S. C. Collins *et al.* (2008) Colour pattern specification in the Mocker Swallowtail
509 *Papilio dardanus*: the transcription factor *invested* is a candidate for the mimicry locus *H*.
510 *Proceedings of the Royal Society B*, **275**, 1181–1188.

511 Clark R, Vogler AP (2009) A phylogenetic framework for wing pattern evolution in the mimetic
512 Mocker Swallowtail *Papilio dardanus*. *Molecular Ecology*, **18**, 3872–3884.

513 Ebersberger I, Strauss S, Haeseler A (2009) HaMStR: Profile hidden markov model based search for
514 orthologs in ESTs. *BMC Evolutionary Biology*, **9**, 1–9.

515 Egea R, Casillas S, Barbadilla A (2008) Standard and generalized McDonald–Kreitman test: a website
516 to detect selection by comparing different classes of DNA sites. *Nucleic Acids Research*, **36**,
517 W157–W162.

518 Fisher RA (1927) On some objections to mimicry theory; statistical and genetic. *Transactions of the*
519 *Royal Entomological Society*, **75**, 269–274.

520 Ford EB (1936) The genetics of *Papilio dardanus* Brown (Lep.). *Transactions of the Royal*
521 *Entomological Society London*, **85**, 435–466.

522 Gillett CPDT, Crampton-Platt A, Timmermans MJTN *et al.* (2014) Bulk de novo mitogenome assembly
523 from pooled total DNA elucidates the phylogeny of weevils (Coleoptera: Curculionoidea).
524 *Molecular biology and evolution*, **31**, 2223–2237.

525 Grabherr MG, Haas BJ, Yassour M *et al.* (2011) Full-length transcriptome assembly from RNA-Seq
526 data without a reference genome. *Nat Biotech*, **29**, 644–652.

527 Hoquet T, Levandowsky M (2016) Utility vs Beauty: Darwin, Wallace and the Subsequent History of
528 the Debate on Sexual Selection. In: *Current Perspectives on Sexual Selection, History,*
529 *Philosophy and Theory of the Life Sciences*, pp. 19–28. Springer Science+Business Media,
530 Dordrecht.

531 Jukes TH, Cantor CR (1969) Evolution of protein molecules. In: *Mammalian Protein Metabolism* (ed
532 Munro H. N). Academic Press, New York.

533 Junier T, Zdobnov EM (2010) The Newick utilities: high-throughput phylogenetic tree processing in
534 the Unix shell. *Bioinformatics*, **26**, 1669–1670.

535 Katoh K, G. Asimenos, H. Toh (2009) Multiple Alignment of DNA Sequences with MAFFT. In: *Methods*
536 *in Molecular Biology. Volume 537* (ed Posada D), pp. 39–64. Humana Press.

537 Kawahara AY, Breinholt JW (2014) Phylogenomics provides strong evidence for relationships of
538 butterflies and moths. *Proceedings of the Royal Society of London B: Biological Sciences*, **281**.

539 Kearse M, Moir R, Wilson A *et al.* (2012) Geneious Basic: an integrated and extendable desktop
540 software platform for the organization and analysis of sequence data. *Bioinformatics*
541 *(Oxford, England)*, **28**, 1647–1649.

542 Komata S, Lin C-P, Iijima T, Fujiwara H, Sota T (2016) Identification of doublesex alleles associated
543 with the female-limited Batesian mimicry polymorphism in *Papilio memnon*. *Scientific*
544 *Reports*, **6**, 34782.

545 Kraaijeveld K (2014) Reversible Trait Loss: The Genetic Architecture of Female Ornaments. *Annual*
546 *Review of Ecology, Evolution, and Systematics*, **45**, 159–177.

547 Kunte K (2008) Mimetic butterflies support Wallace’s model of sexual dimorphism. *Proceedings of*
548 *the Royal Society B-Biological Sciences*, **275**, 1617–1624.

549 Kunte K (2009) The diversity and evolution of Batesian mimicry in *Papilio swallowtail* butterflies.
550 *Evolution*, **63**, 2707–2716.

551 Kunte K, Zhang W, Tenger-Trolander A *et al.* (2014) doublesex is a mimicry supergene. *Nature*,
552 **507**, 229–232

553 Lanfear R, Calcott B, Ho SYW, Guindon S (2012) Partitionfinder: combined selection of partitioning
554 schemes and substitution models for phylogenetic analyses. *Molecular biology and*
555 *evolution*, **29**, 1695–1701.

556 Librado P, Rozas J (2009) DnaSP v5: a software for comprehensive analysis of DNA polymorphism
557 data. *Bioinformatics*, **25**.

558 Li W, Godzik A (2006) Cd-hit: a fast program for clustering and comparing large sets of protein or
559 nucleotide sequences. *Bioinformatics*, **22**, 1658–9.

560 Li H, Handsaker B, Wysoker A *et al.* (2009) The Sequence Alignment/Map format and SAMtools.
561 *Bioinformatics (Oxford, England)*, **25**, 2078–2079.

562 MacManes MD, Eisen MB (2013) Improving transcriptome assembly through error correction of
563 high-throughput sequence reads. *PeerJ*, e113.

564 Margulies M, Egholm M, Altman WE *et al.* (2005) Genome sequencing in microfabricated high-
565 density picolitre reactors. *Nature*, **437**, 376–380.

566 McDonald JH, Kreitman M (1991) Adaptive protein evolution at the Adh locus in *Drosophila*. *Nature*,
567 **351**, 652–654.

568 Nei M, Gojobori T (1986) Simple methods for estimating the numbers of synonymous and
569 nonsynonymous nucleotide substitutions. *Molecular Biology and Evolution*, **3**, 418–426.

570 Nicholson AJ (1927) A new theory of mimicry in insects. *Australian Journal of Zoology*, **5**, 10–104.

571 Nielsen R (2005) Molecular signatures of natural selection. *Annual Review Of Genetics*, **39**, 197–218.

572 Nijhout HF (2003) Polymorphic mimicry in *Papilio dardanus*: mosaic dominance, big effects, and
573 origins. *Evolution and Development*, **5**, 579–592.

574 Nishikawa H, Iijima T, Kajitani R *et al.* (2015) A genetic mechanism for female-limited Batesian
575 mimicry in *Papilio* butterfly. *Nat Genet*, **47**, 405–409.

576 Oliver JC, Monteiro A (2011) On the origins of sexual dimorphism in butterflies. *Proceedings of the*
577 *Royal Society of London B: Biological Sciences*, **278**, 1981–1988.

578 Paradis E, Claude J, Strimmer K (2004) APE: Analyses of Phylogenetics and Evolution in R language.
579 *Bioinformatics*, **20**, 289–290.

580 Parra G, Bradnam K, Korf I (2007) CEGMA: a pipeline to accurately annotate core genes in eukaryotic
581 genomes. *Bioinformatics*, **23**, 1061–1067.

582 Parra G, Bradnam K, Ning Z, Keane T, Korf I (2009) Assessing the gene space in draft genomes.
583 *Nucleic Acids Research*, **37**, 289–297.

584 Regier JC, Shultz JW, Zwick A *et al.* (2010) Arthropod relationships revealed by phylogenomic analysis
585 of nuclear protein-coding sequences. *Nature*, **463**, 1079–U98.

586 Schliep KP (2011) phangorn: phylogenetic analysis in R. *Bioinformatics*, **27**, 592–593.

587 Schmieder R, Edwards R (2011) Quality control and preprocessing of metagenomic datasets.
588 *Bioinformatics*, **27**, 863–864.

589 Stamatakis A (2006) RAxML-VI-HPC: Maximum likelihood-based phylogenetic analyses with
590 thousands of taxa and mixed models. *Bioinformatics*, **22**, 2688–2690.

591 Tamura K, Stecher G, Peterson D, Filipowski A, Kumar S (2013) MEGA6: Molecular Evolutionary Genetics
592 Analysis version 6.0. *Molecular biology and evolution*, **30**, 2725–2729.

593 Thompson MJ, Timmermans MJTN (2014) Characterising the phenotypic diversity of *Papilio*
594 *dardanus* wing patterns using an extensive museum collection. *PLoS ONE*, **9**, e96815.

595 Thompson MJ, Timmermans MJ, Jiggins CD, Vogler AP (2014) The evolutionary genetics of highly
596 divergent alleles of the mimicry locus in *Papilio dardanus*. *BMC Evolutionary Biology*, **14**, 1–
597 13.

598 Thompson MJ, Vane-Wright RI, Timmermans MJTN (2011) HYBRID ORIGINS: DNA TECHNIQUES
599 CONFIRM THAT *PAPILIO NANDINA* IS A SPECIES HYBRID (PAPILIONIDAE). *Journal of the*
600 *Lepidopterists Society*, **65**, 199–201.

601 Timmermans MJTN, Baxter SW, Clark R *et al.* (accepted) Comparative genomics of the mimicry
602 switch in *Papilio dardanus*. *Proceedings of the Royal Society B-Biological Sciences*.

603 Timmermans MJTN, Baxter SW, Clark R *et al.* (2014a) Comparative genomics of the mimicry switch in
604 *Papilio dardanus*. *Proceedings of the Royal Society B-Biological Sciences*, **281**.

605 Timmermans MJTN, Lees DC, Simonsen TJ (2014b) Towards a mitogenomic phylogeny of
606 Lepidoptera. *Molecular phylogenetics and evolution*, **79**, 169–178.

607 Turner JRG (1984) Mimicry: the palatability spectrum and its consequences. In: *The biology of*
608 *butterflies* (eds Vane-Wright RI, P. R. Ackery), pp. 141–161. Academic Press, New York.

609 Vane-Wright RI (1971) The systematics of *Drusillopsis* Oberthür (Satyrinae) and the supposed
610 amathusiid *Bigaena* van Eecke (Lepidoptera: Nymphalidae), with some observations on
611 Batesian mimicry. *Transactions of the Royal Entomological Society of London*, **123**, 97–123.

612 Vane-Wright RI, D. C. Raheem, A. Cieslak, A. P. Vogler (1999) Evolution of the mimetic African
613 swallowtail butterfly *Papilio dardanus*: molecular data confirm relationships with *P. phorcas*
614 and *P. constantius*. *Biological Journal of the Linnean Society*, **66**, 215–229.

615 Wallace AR (1865) I. On the Phenomena of Variation and Geographical Distribution as illustrated by
616 the Papilionidæ of the Malayan Region. *Transactions of the Linnean Society of London*, **25**, 1–
617 71.

618 Wernersson R (2005) FeatureExtract--extraction of sequence annotation made easy. *Nucleic acids*
619 *research*, **33**, W567–569.

620 Yang X, Dorman KS, Aluru S (2010) Reptile: representative tiling for short read error correction.
621 *Bioinformatics*, **26**, 2526–2533.

622 Zakharov EV, Caterino MS, Sperling FAH (2004) Molecular phylogeny, historical biogeography, and
623 divergence time estimates for swallowtail butterflies of the genus *Papilio* (Lepidoptera :
624 Papilionidae). *Systematic Biology*, **53**, 193–215.

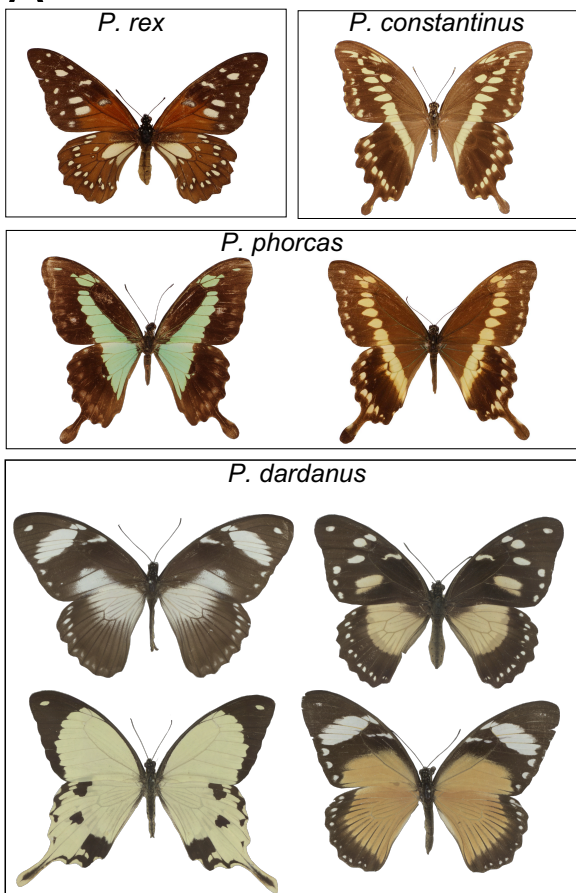
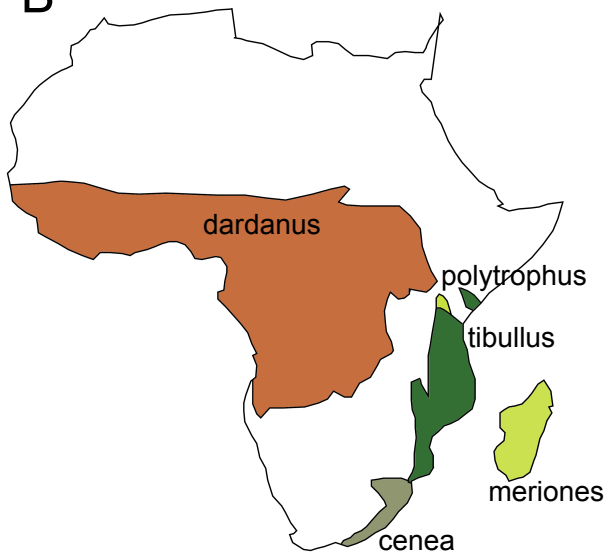
625 Zhang W, Kunte K, Kronforst MR (2013) Genome-Wide Characterization of Adaptation and
626 Speciation in Tiger Swallowtail Butterflies Using De Novo Transcriptome Assemblies.
627 *Genome Biology and Evolution*, **5**, 1233–1245.

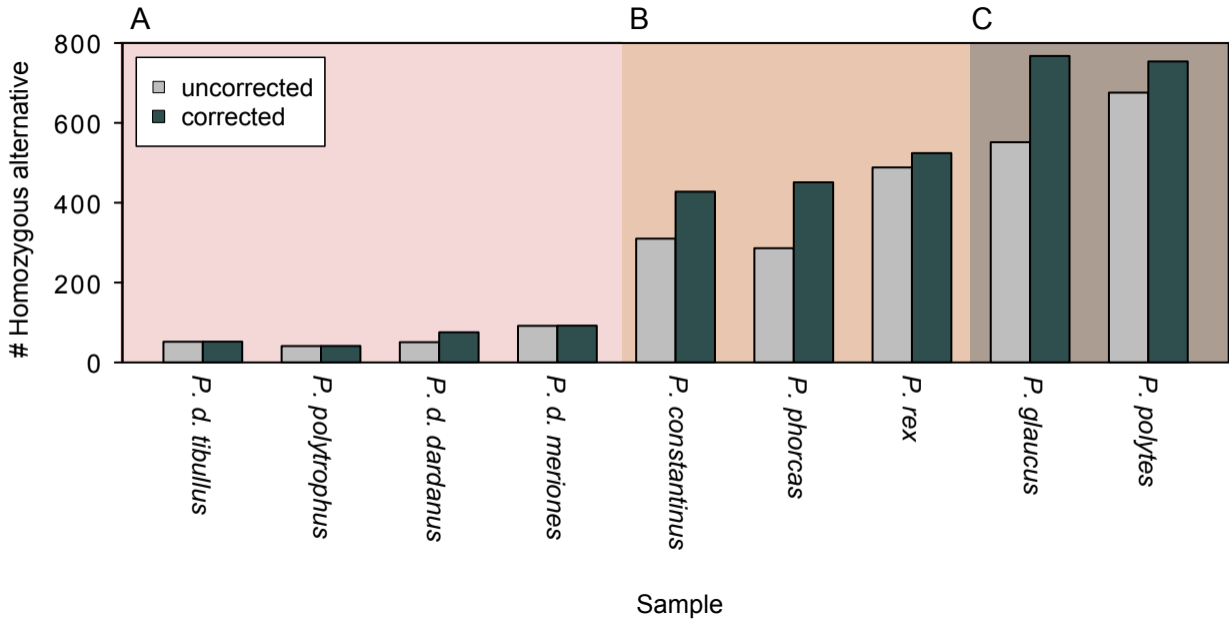
628 Zwick A, Regier JC, Zwickl DJ (2012) Resolving Discrepancy between Nucleotides and Amino Acids in
629 Deep-Level Arthropod Phylogenomics: Differentiating Serine Codons in 21-Amino-Acid
630 Models. *PLoS ONE*, **7**.

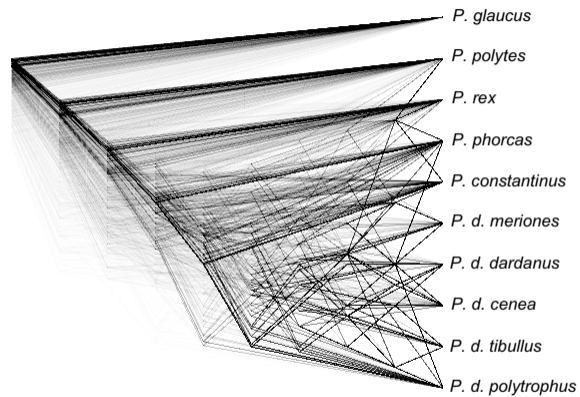
631

(Sub)species	Country	Female phenotype	N	to <i>P. rex</i> (r) or <i>P. constantinus</i> (c)	Non-synonymous divergence	Net non-synonymous divergence	Synonymous divergence	Net synonymous divergence	MK test				
									Synonymous Divergence	Synonymous Polymorphism	Non-synonymous Divergence	Non-synonymous Polymorphism	Fisher's exact test P-value
<i>P. dardanus polytrophus</i> *	Kenya	Polymorphic - mimetic	73	r	0.025	0.016	0.278	0.234	20.89	36	3.01	36	0.001
				c	0.030	0.019	0.246	0.191	14.42	42	4.03	41	0.031
<i>P. dardanus polytrophus</i>	Kenya	Polymorphic - mimetic	67	r	0.022	0.016	0.272	0.236	23.34	31	3.01	27	0.001
				c	0.028	0.019	0.243	0.195	16.78	37	4.03	33	0.023
<i>P. phorcas</i>	Kenya	Polymorphic. not mimetic	15	r	0.032	0.027	0.328	0.273	23.34	31	8.13	10	0.887
				c	0.032	0.025	0.267	0.200	16.78	37	7.1	16	0.967
<i>P. dardanus dardanus</i> **	Ghana	Monomorphic - mimetic	13	r	0.020	0.015	0.254	0.226	21.97	18	4.03	11	0.062
				c	0.025	0.018	0.232	0.192	19.34	24	5.05	17	0.086
<i>P. dardanus meriones</i>	Madagascar	Monomorphic - not mimetic	13	r	0.021	0.019	0.282	0.251	26.14	25	6.07	5	0.821
				c	0.026	0.021	0.258	0.215	19.34	31	6.07	11	0.834

Table 1: Distances and McDonald-Kreitman test for the *engrailed* locus. Results from analyses with *P. rex* and *P. constantinus* are given for each (sub-)species. Divergence is defined as the number of (non-)synonymous differences per (non-)synonymous site. For the McDonald-Kreitman tests (MK test) synonymous and non-synonymous differences (fixed and variable) after Jukes and Canter (Jukes & Cantor 1969) correction are given. N) Number of specimen. (*) Data from Timmermans *et al.* 2014). (**) Female form *P. dardanus f. dionysos* occurs at low frequency in this population.

A**B**



A**B**